

# Measurements of Velocity Profiles in the Aqueous Boundary Layer at a Wind-Driven Water Surface

*Jochen Dieter*<sup>1,2</sup>, *Frank Hering*<sup>2</sup>, *Roland Bremeyer*<sup>2</sup>,  
*and Bernd Jähne*<sup>1,2,3</sup>

<sup>1</sup>Scripps Institution of Oceanography, Physical Oceanography Res. Div.  
La Jolla, CA 92093-0230, USA, email: [jdieter@ucsd.edu](mailto:jdieter@ucsd.edu)

<sup>2</sup>Institute for Environmental Physics, University of Heidelberg  
Im Neuenheimer Feld 366, 69120 Heidelberg, Germany

<sup>3</sup>Interdisciplinary Center for Scientific Computing, University of Heidelberg  
Im Neuenheimer Feld 368, 69120 Heidelberg, Germany

## Abstract

A two-dimensional flow-visualization technique for the investigation of wind-induced currents in the boundary layer beneath the water surface is presented. Experiments were conducted at the Heidelberg wind-wave facility at conditions where either wave motion was suppressed by surfactants or was not present because of low wind speeds. A PIV setup enables the calculation of flow vector fields and velocity profiles in an area of 4 mm beneath the interface. Parameters of this layer, such as the friction velocity were deduced from these profiles.

## 1 Introduction

The investigation of micro-scale turbulence near the free air/sea interface is important to understand wind-driven small-scale transport processes across the water surface. Flow measurements at different scales on both sides of the interface reveal information about the turbulent transport of momentum and the turbulent dissipation of energy as well as the influence of waves on these processes.

Of particular interest is the layer down to the first millimeter beneath the water surface, where viscous transport processes exceed the turbulent. Most parameters of the transport processes in this layer, can be deduced from mean velocity profiles in that layer. Measurements in this part of the flow are very rare, since the velocities are high in respect to the area of interest. The presence of waves makes the observation even more difficult. Therefore hardly any measurements of this area are available, except some pioneer work by *Okuda* [1992] for the air side and *Sivakumar* [1984] for the water side layer.

A setup for high-resolution *particle image velocimetry (PIV)*-measurements in the Heidelberg wind-wave flume was developed. Investigations of the flow, with wave motion being suppressed by the use of surfactants

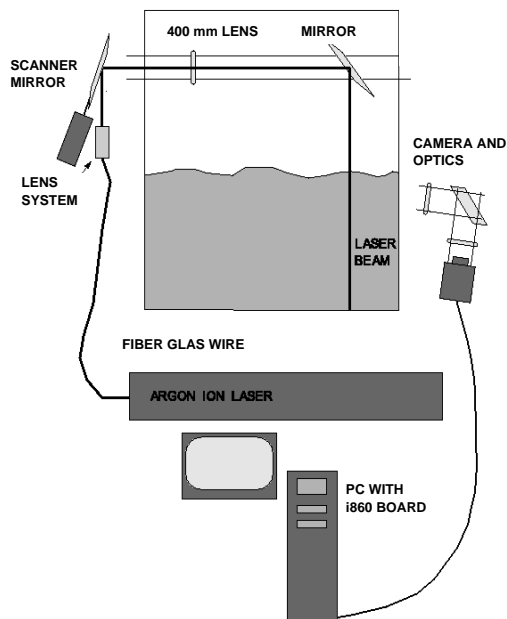


Figure 1: The setup used for PIV-measurements in the viscous boundary layer.

(Triton X100), were made. Low wave amplitudes at low wind speed make measurements with no surfactants also feasible.

Eulerian vector fields were extracted by a multi-grid PIV algorithm, especially designed for the processing of large displacements vectors. Velocity profiles and parameters of the viscous boundary layer, the friction velocity and the surface velocity are deduced from these vector fields.

## 2 Experimental Setup

Experiments are conducted at the Heidelberg wind-wave flume, with a setup very similar to one developed by *Münsterer and Jähne* [1995] for the acquisition of gas exchange rates. The circular Heidelberg facility provides the possibility to investigate events in the middle of a 35cm broad channel through windows in the flume wall from outside. Thus it is possible to place delicate equipment very close to the observed area with no interaction between the air/water stream and the optical instrumentation. This feature enables a setup of a high resolution optic beneath the water level of the flume. Two achromatic 200 mm lenses picture an area of 4 mm  $\times$  4 mm on a 256  $\times$  256 pixel CCD-array of a high-speed non-interlaced camera (Dalsa CA-D1). This yields a spatial resolution of 16  $\mu$ m and a frame rate of 200

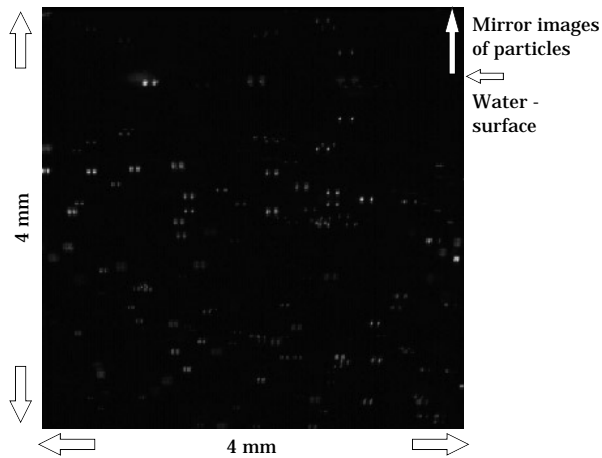


Figure 2: Image of particles in the viscous boundary layer taken at a wind speed of 1 m/s. The velocity decrease with the water depth is easy to verify by the distance of particle image pairs. It is also easy to determine the water surface. All particle images above the water surface are mirror images reflected at the interface.

frames/sec. The angle between the optical axis of this image acquisition equipment and the water surface was chosen  $8^\circ$  to avoid disturbances of the image by the interface outside the area of interest.

The flow was visualized by small seeding particles produced by electrolysis. Hydrogen bubbles are generated on the cathode, of a tungsten wire of  $50\ \mu\text{m}$  diameter. In order to get a sufficient number of particles in the observed volume, the wire is placed close (about 10 cm upstream) to the area of interest. There is a potential voltage drop of 60 V between the wire and the anode at 10 cm distance at the flume wall. Since the flume is filled with deionized water, 0.15 g/l  $\text{NaSO}_4$  is added to enable electrolysis [Oertel and Oertel, 1989].

For illumination a  $\text{TEM}_{00}$  1 W argon ion laser (American Laser Corp., model 909) with a wavelength of 488 nm is used. The light is guided through a fiber glass wire. A lens system at the end of the wire and an additional 400 mm lens enables an adjustable beam diameter between  $60\ \mu\text{m}$  and 2 mm. Corresponding to the depth of focus of  $400\ \mu\text{m}$  a beam diameter of about  $300\ \mu\text{m}$  is used. A scanner mirror generates a light sheet, which is directed by a second mirror into the water (see Figure 1). The scanner mirror is driven by a sinusoidal signal, that also synchronizes the camera each period. This yields two dots for every particle in one image frame. The light sheet is chosen larger than the picture frame. Although intensity is lost, a nearly linear laser beam velocity in the picture area is gained.

The camera is connected to a digital camera interface of a Hyperspeed XPI-i860 board. The images are stored in the RAM of the board during the

measurement. 34 MByte RAM allow 450 pictures ( $\equiv 2$  s) to be taken consecutively.

### 3 Image Processing for PIV

Two-dimensional flow fields from sequential images of seeding particles in the flow are extracted with a Particle Image Velocimetry (PIV) algorithm. In contrary to particle based algorithms, as for example Particle Tracking Velocimetry (PTV), where special characteristics of the image of one particle is used to solve the correspondence problem, in PIV the characteristics of groups of particles is taken as standard for the calculation of displacement vectors (see also *Adrian* [1991], *Willert and Gharib* [1991]). Therefore the pattern created by particle images in a small part of the whole frame taken at the time  $\tau$  was correlated to the next frame of the sequence taken at  $\tau + \Delta t$ . The mean velocity in this two-dimensional area is calculated dividing the shift of that pattern by the time  $\Delta t$  given by frame rate of the image acquiring system. The vector displacement was evaluated by using the spatial discrete correlation of these two areas.

The coordinates of the maximum of the correlation function is the most probable spatial shift vector and yields the mean displacement vector of the particles in the window. Typically a square area of  $32 \times 32$  pixels is chosen as the matching window size for PIV measurements on digital images. The crosscorrelation is calculated in Fourier space using a discrete Fourier transformation done by a fast fourier algorithm FFT.

The detection of the peak in the cross correlation is often difficult, because of noise in the correlation function. In addition the peak tends to broaden, due to the gaussian form of the particles and from velocity gradients in the picture area. On the other hand this broadening is used for sub pixel accuracy processing via a center of mass algorithm. The noise results from:

- noise in the picture areas,
- three dimensional movement in and out of the light sheet,
- two dimensional movement of particles beyond the interrogation window,
- other particle patterns that randomly match up with the sampled picture area.

In other words sometimes the detected peak did not correlate to the real displacement vector. The quotient of the highest peak with the next lower is used as a measure of confidence for the results [*Keane and Adrian*, 1990]. Displacements larger than half the interrogation window can not be separated from displacements in the opposite direction, when the correlation is calculated in the Fourier space (Nyquist theorem).

Corresponding to the relatively high velocities of 10 cm/s in the boundary

layer spatial displacements up to 32 pixels are expected. In order to enable the evaluation of these shift vectors a multi grid algorithm was developed [Dieter et. al., 1994]. It divides the processing in two steps. First an estimate of the displacement vector is evaluated. This processing step was done on higher levels (in this case on the second level) of a Gaussian pyramid of the image [Jähne, 1995]. The estimate is used to match the second window over the first. Thus it is possible to calculate displacement vectors of up to 32 pixel, without loosing resolution of the vector field.

## 4 Results

The next step is the calculation of the water flow velocity as a function of the water depth. These *velocity profiles* are computed by averaging over all horizontal (parallel to the main wave propagation) velocity components and image sequences of two seconds (Figure 3). Centrifugal forces, which are present in the Heidelberg wind/wave flume because of its circular shape, induce secondary flows perpendicular to the main flow direction. Thus the form of the profiles is not logarithmic. An Airy-Function, as predicted by the *surface renewal model*, is used to fit the velocity profiles. There are two kinds of transport processes present in the boundary layer: diffusive and turbulent transport. The second process is described in the surface renewal model by a probability  $\lambda$  that turbulences reach into the boundary layer at a water depth  $h$ . This is normally done by using the power  $p$  of  $h$ .  $p$  is a real number and  $p \geq 0$ .

$$\lambda = \gamma_p h^p. \quad (1)$$

$\gamma_p$  denotes a constant. The case  $p = 0$  leads to the classic surface renewal model [Higbie, 1935; Münnich and Flothmann, 1975], often used to describe transport processes in the mass boundary layer at a wavy interface. The flow at a smooth water surface, as examined in experiments presented in this paper, is very similar to currents at a plane wall. Therefore  $p$  is set to one, so that  $\lambda$  is proportional to the water depth and no turbulences are present at the water surface. Therefore the solution of the transport equation is the Airy Function (Figure 3, right, small graphic):

$$u(h) = \frac{(u_{Wo} - u_{Bulk})}{Ai(0)} Ai \left( \frac{Ai(0)}{h \sqrt{\gamma_p / \nu} Ai'(0)} \right) + u_{Bulk}. \quad (2)$$

$Ai(0)$  and  $Ai'$  are constant, and  $u_{Wo}$ ,  $u_{Bulk}$  are velocities at the surface and far away from the interface.  $\nu$  is the viscosity of water.

The *surface velocities* extrapolated with the Airy Function from PIV-data are compared to direct surface velocity measurements as obtained by Reinelt [1994] using an imaging active IR technique (Figure 4, left). The friction velocity measured in Heidelberg wind/wave flume and by Sivakumar in a linear

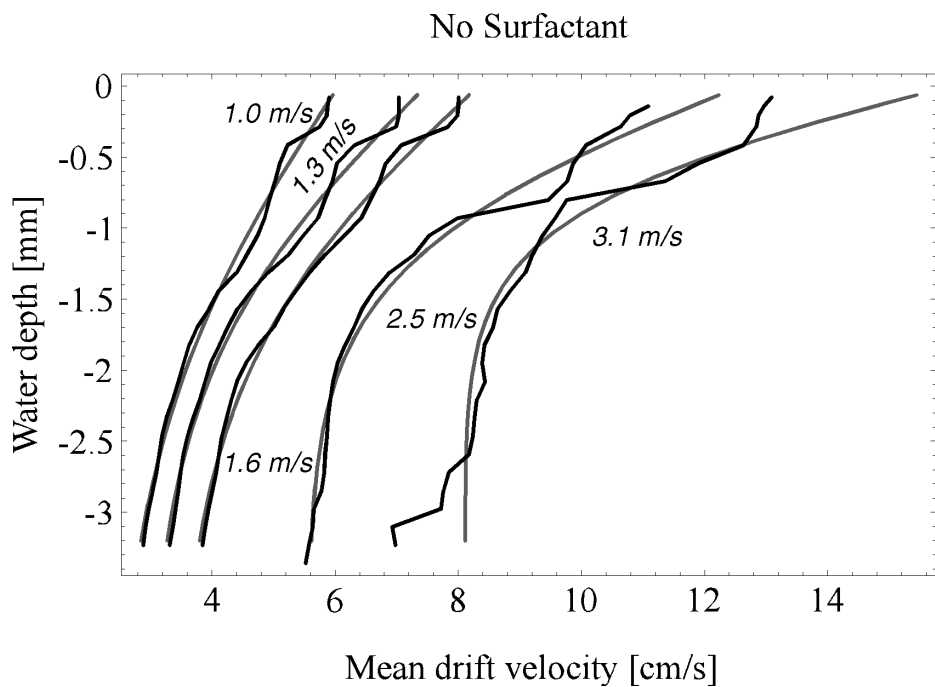
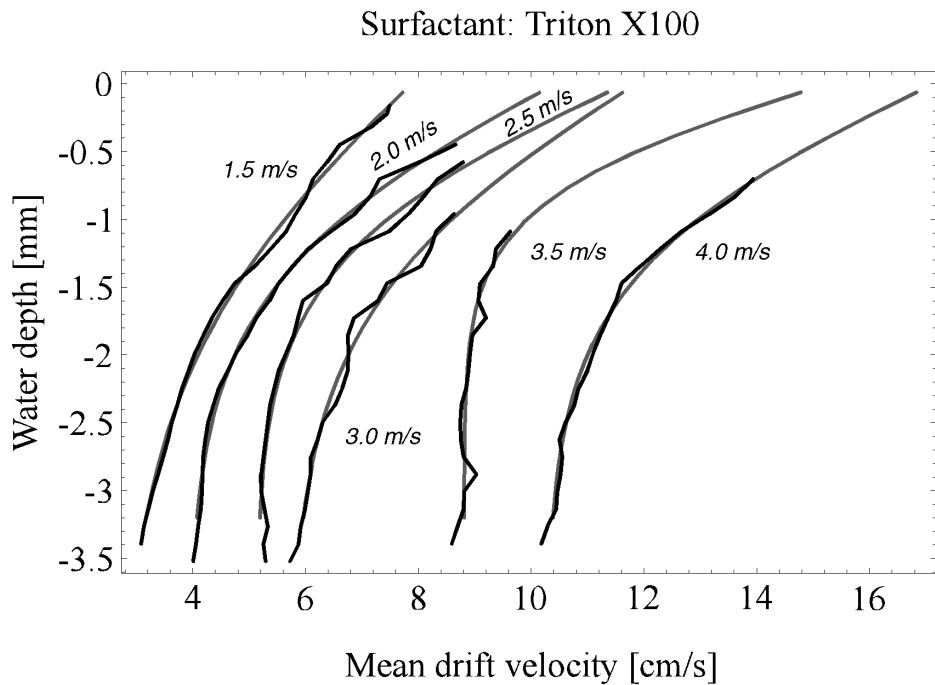


Figure 3: Velocity profiles in the aqueous viscous boundary layer, measured at the Heidelberg circular wind/wave flume. The Airy-Functions fitted in the profiles are shown as gray plots.

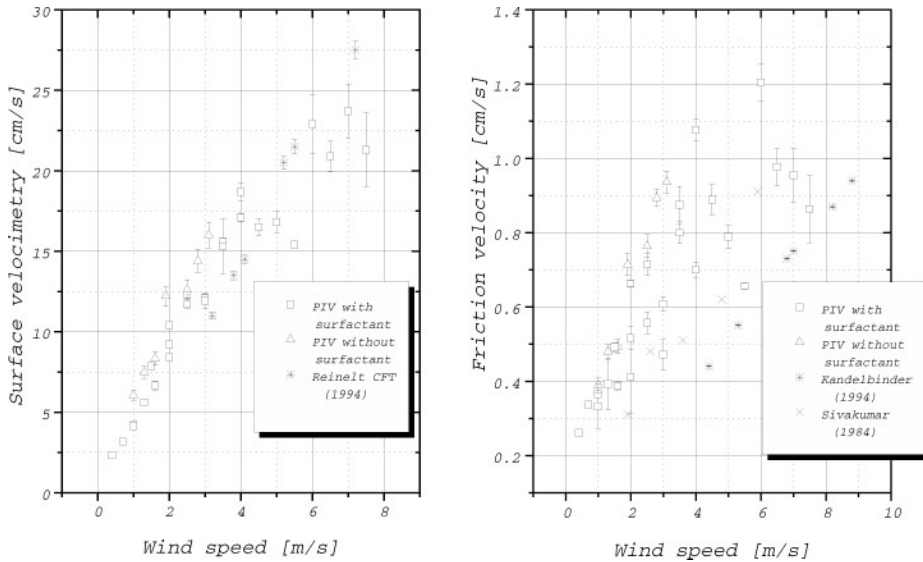


Figure 4: Left: Surface velocity as measured in the Heidelberg wind-wave flume. Right: Friction velocity measured in Heidelberg wind/wave flume and by Sivakumar in a linear wind wave tank of the University Newcastle.

wind wave tank of the University Newcastle are shown in Figure 4, right. Experiments by *Kandelbinder* [1994] were made using a momentum balance method in the Heidelberg flume. The lower values of the measurements by *Kandelbinder* can be explained, because the average over a much larger area close to the middle of the channel, where wind and water speed are lower, was taken into account. *Sivakumar* [1984] acquired his friction velocity data by flow measurements with floats near the interface and hot films away from the surface. Contrary to the other experiments, this data was taken at a wavy interface.

## 5 Conclusions

We successfully demonstrated a high-resolution PIV-flow visualization system to measure vertical velocity profiles within the viscous boundary layer. The results, are comparable to those gained by other techniques. This research is a first step in applying advanced imaging techniques for quantitative flow visualization techniques in the aqueous viscous boundary layer at a wavy interface. The next steps will be:

1. Improving the spatial resolution for measurements at higher wind speeds.
2. Incorporation of the optical system into a wave follower for measurements at a wavy interface.

## References

- Adrian, R. J., Particle-Imaging Techniques for Experimental Fluid Mechanics, *Ann. Rev. Fluid Mech.*, 23, 261-304, 1991
- Dieter, J., R. Bremeyer, F. Hering, and B. Jähne, Flow measurements close to the free air/sea interface, *Proceedings to the Seventh International Symposium on Applications of Laser Techniques to Fluid Mechanics*, 1994
- Higbie, R., The rate of absorption of a pure gas into a still liquid during short periods of exposure, *Trans. A.I. Ch. E.* 31, 365-389, 1935
- Jähne, B., *Digital Image Processing, Concepts, Algorithms and Scientific Applications*, pp. 289-293 and 200-205, 3rd edition, Springer-Verlag, Berlin, 1995
- Kandelbinder, T., *Gasaustauschmessungen mit Sauerstoff*, Diploma thesis, Universität Heidelberg, 1994
- Keane, D. K., and R. J. Adrian, Optimization of particle image velocimeters. Part 1: Double pulsed systems, *Meas. Sci. Technol.* 1, 1202-1215, 1990
- Münnich, K. O., and D. Flothmann, Gas exchange in relation to other air-sea interaction phenomena, *SCOR Workshop on Air/Sea Interaction Phenomena*, Miami, Dec 8-12, 1975
- Münsterer, T., and B. Jähne, A Fluorescence Technique to Measure Concentration Profiles in the Aqueous Mass Boundary Layer, in *The Air-Sea Interface*, M. A. Donelan, W. H. Hui, W. J. Plant, eds. The University of Toronto Press, Toronto, 1995, in press.
- Oertel, H. sen., and H. Oertel, jun., *Strömungsmesstechnik*, 413-415, G. Braun, Karlsruhe, 1989
- Okuda, K., Internal Flow Structure of Short Wind Waves, Part 1. On the Internal Vorticity Structure, *Journal of the Oceanographical Soc. of Japan*, 44, 28-42, 1982
- Reinelt, S., *Bestimmung der Transfergeschwindigkeit mittels CFT mit Wärme als Tracer*, Diploma thesis, Universität Heidelberg, 1994
- Sivakumar, M., Reaeration and wind induced turbulence shear in a contained water body, in: *Gas transfer at water surfaces*, W. Brutsaert and G. H. Jirka eds., Reidel, Dordrecht, 369-377, 1984
- Willert, C., and M. Gharib, Digital particle image Velocimetry, *Exp. in Fluids*, 10, 181-193, 1991